

Different Cellular and Genetic Basis of Noise-Related Endocochlear Potential Reduction in CBA/J and BALB/cJ Mice

KEVIN K. OHLEMILLER^{1,3}, ALYSON D. ROSEN³, ERIN A. RELLINGER³, SCOTT C. MONTGOMERY², AND PATRICIA M. GAGNON¹

¹*Department of Otolaryngology, Washington University School of Medicine, 660 S. Euclid, St. Louis, MO 63110, USA*

²*Department of Otolaryngology, Saint Louis University School of Medicine, St. Louis, MO, USA*

³*Program in Audiology and Communication Sciences, Washington University School of Medicine, St. Louis, MO, USA*

Received: 28 July 2010; Accepted: 20 September 2010; Online publication: 5 October 2010

ABSTRACT

The acute and permanent effects of noise exposure on the endocochlear potential (EP) and cochlear lateral wall were evaluated in BALB/cJ (BALB) inbred mice, and compared with CBA/J (CBA) and C57BL/6 (B6) mice. Two-hour exposure to broadband noise (4–45 kHz) at 110 dB SPL leads to a ~50 mV reduction in the EP in BALB and CBA, but not B6. EP reduction in BALB and CBA is reliably associated with characteristic acute cellular pathology in stria vascularis and spiral ligament. By 8 weeks after exposure, the EP in CBA mice has returned to normal. In BALBs, however, the EP remains depressed by an average ~10 mV, so that permanent EP reduction contributes to permanent threshold shifts in these mice. We recently showed that the CBA noise phenotype in part reflects the influence of a large effect quantitative trait locus on Chr. 18, termed *Nirep* (Ohlemiller et al., *Hear Res* 260:47–53, 2010b). While CBA “EP susceptibility” alleles are dominant to those in B6, examination of (B6×BALB) F1 hybrid mice and (F1×BALB) N2 backcross mice revealed that noise-related EP reduction and associated cell pathology in BALBs are inherited in an autosomal recessive manner, and are dependent on multiple genes. Moreover, while N2 mice formed from B6 and CBA retain strong correspondence between acute EP reduction, ligament pathology, and stria pathology, N2s formed from B6 and BALB include subsets that

dissociate pathology of ligament and stria. We conclude that the genes and cascades that govern the very similar EP susceptibility phenotypes in BALB and CBA mice need not be the same. BALBs appear to carry alleles that promote more pronounced long term effects of noise on the lateral wall. Separate loci in BALBs may preferentially impact stria versus ligament.

Keywords: stria vascularis, spiral ligament, spiral limbus, Reissner’s membrane, fibrocytes, C57BL/6, noise-induced hearing loss, presbycusis

INTRODUCTION

From decades of study of noise-induced hearing loss (NIHL), some consensus has emerged concerning both the reversible cochlear changes underlying the transient component of hearing loss, and irreversible changes associated with permanent hearing loss. Reversible changes may include altered spatial relations within the organ of Corti (Beagley 1965; Harding et al. 1992; Nordmann et al. 2000), injury to hair cell stereocilia (Liberman and Kiang 1978; Liberman and Mulroy 1982; Liberman and Dodds 1984), and transient depression of the endocochlear potential (EP) (Syka et al. 1981). Critical irreversible changes (those accounting for permanent hearing loss) have appeared concentrated in the organ of Corti. These include hair cell loss and non-lethal hair cell injury (e.g., Covell 1953; Johnson and Hawkins 1976; Hamernik et al. 1989; Ou et al. 2000b; Wang et al. 2002) as well as newly recognized delayed and progressive

Correspondence to: Kevin K. Ohlemiller · Department of Otolaryngology · Washington University School of Medicine · 660 S. Euclid, St. Louis, MO 63110, USA. Telephone: +1-314-7477179; fax: +1-314-7477230; email: kohlemiller@wustl.edu

injury to afferent neurons (Kujawa and Liberman 2009). The latter may not contribute to hearing loss per se, but rather to supra-threshold deficits. Permanent EP reduction has not generally been held to be a common contributor to permanent NIHL. EP reduction by noise may reflect two very different mechanisms, depending on the severity of the noise and the model. Traumatic noise that tears Reissner's membrane or breaches the reticular lamina can reduce the EP by eliminating the required ion gradients. Reversible EP reduction by noise that does not violate the boundaries of scala media has been demonstrated in some mouse strains (CBA/J and CBA/CaJ) and not others (C57BL/6J, or B6), and thus to reflect genetically modifiable factors intrinsic to the lateral wall (Hirose and Liberman 2003; Ohlemiller and Gagnon 2007). Following a single moderate noise exposure (4–45 kHz, 110 dB sound pressure level (SPL), 2 h), CBA/J mice (henceforth CBA) show a 40–50 mV reversible EP reduction that is reliably accompanied by certain forms of stria and ligament pathology. For the same exposure, B6 mice show neither EP reduction nor significant lateral wall pathology. We recently showed that differences in the vulnerability of the EP between CBA and B6 mice in part reflect the influence of a major effect quantitative trait locus (QTL) on Chr. 18, termed *Nirep* (Ohlemiller et al. 2010b). *Nirep* was found to account for about 12% of EP variance, with an effect size of ~19 mV. Here we show that, like CBAs, BALB/cJ (BALB) mice also show EP reduction following the same noise exposure. Although the acute cellular pathology associated with EP reduction in BALBs is quite similar to that in CBAs, BALBs show several major differences. Among these are a different mode of inheritance, clear involvement of multiple loci, and dissociability of injury to stria vascularis and spiral ligament. Most significantly, unlike CBA the EP remains somewhat depressed in BALBs 8 weeks after noise exposure. Thus, BALBs appear to carry alleles that promote long term effects of noise on the cochlear lateral wall. Similar alleles and influences may operate in the human cochlea, and could impact the long term stability of NIHL and the manifestation of presbycusis.

MATERIALS AND METHODS

Animals

All procedures were approved by the Washington University Institutional Animal Care and Use Committee. The basic procedure involved exposing inbred, hybrid, and backcross mice one time to broadband noise followed by hearing assessment, recording of the EP, and sacrifice for histology either 1–3 h, 24 h, or 8 weeks

after exposure. Mice were 3–4 months of age at the time of exposure. All groups were roughly evenly balanced by gender and no gender effects were evident in any of the data we present. Mice were purchased directly from The Jackson Laboratory (JAX) or were derived from breeders purchased from JAX. Subjects included 66 BALB/cJ, 29 CBA/J (CBA), and 26 C57BL/6J (B6), and 27 B6.CAST-*Cdh23*^{CAST} (B6.CAST) mice. Because we previously showed that the effect of noise on the EP was the same in B6 and B6.CAST mice (that is, the *Cdh23*^{ahl} allele does not play a role) (Ohlemiller and Gagnon 2007), data from B6 and B6.CAST were combined for assessment of acute threshold and EP changes. Also included were data from 36 (B6×CBA) F1 hybrids, 55 (B6×BALB) F1 hybrids and 56 [(B6×BALB)×BALB] N2 backcross mice.

Noise exposure

Noise exposures were performed in a foam-lined, single-walled soundproof room. The noise exposure apparatus consisted of a 21×21×11 cm wire cage mounted on a pedestal inserted into a B&K 3921 turntable. To ensure a uniform sound field, the cage was rotated at 1 revolution/80 s within a 42×42 cm metal frame. A Motorola KSN1020A piezo ceramic speaker (four total) was attached to each side of the frame. Opposing speakers were displaced so as not to lie on the same axis and driven by separate channels of a Crown D150A power amplifier. Broadband noise was generated by General Radio 1310 generators and band-passed at 4–45 kHz by Krohn–Hite 3550 filters. Noise levels at various points in the exposure cage, measured using a B&K 4135 1/4 inch microphone in combination with a B&K 2231 sound level meter, ranged from 110–113 dB SPL. Mice were exposed in pairs for 2 h.

CAP recording

Compound action potential (CAP) recordings were conducted as terminal procedures, so that each animal was assessed once immediately prior to sacrifice. Animals were anesthetized (60 mg/kg sodium pentobarbital, IP) and positioned ventrally in a custom headholder. Core temperature was maintained at 37.5±1.0°C using a thermostatically controlled heating pad in conjunction with a rectal probe (Yellow Springs Instruments Model 73A). An incision was made along the midline of the neck and soft tissues were bluntly dissected and displaced laterally to expose the trachea and animal's left bulla. A tracheostomy was then made and the musculature over the bulla was cut posteriorly to expose the bone overlying the round window. Using a hand drill, a small hole was made over the round window. The recording

electrode was a modified platinum needle electrode (Grass) insulated with epoxy except for the tip, which was inserted into round window antrum using a micromanipulator. Additional platinum electrodes inserted into the neck musculature and hind leg served as reference and ground, respectively. Electrodes were led to a Grass P15 differential amplifier (100–3,000 Hz, $\times 100$), then to a custom amplifier providing another $\times 1,000$ gain, then digitized at 30 kHz using a Cambridge Electronic Design Micro1401 in conjunction with SIGNAL™ and custom signal averaging software operating on a 120 MHz Pentium PC. Sinewave stimuli generated by a Hewlett Packard 3325A oscillator were shaped by a custom electronic switch to 5 ms total duration, including 1 ms rise/fall times. The stimulus was amplified by a Crown D150A power amplifier and output to a KSN1020A piezo ceramic speaker located 7 cm directly lateral to the left ear. Stimuli were presented freefield and calibrated using a B&K 4135 1/4 inch microphone placed where the mouse's ear would normally be for recording. Toneburst stimuli at each frequency and level were presented 100 times at 3/s. The minimum sound pressure level required for visual detection of a response (N_1) was determined at 5, 10, 20, 28.3, and 40 kHz, using a 5 dB minimum step size.

Endocochlear potential recording

The EP was measured using a ventral approach immediately after CAP recording. Using a fine drill, a hole was made in the left cochlear capsule directly over scala media of the lower basal turn. Under normal conditions there exists in mouse cochleae a 9–10 mV EP gradient favoring the base (Ohlemiller et al. 2006). When the EP is acutely reduced by noise (Ohlemiller and Gagnon 2007), or chronically reduced with age (Ohlemiller et al. 2010a), this gradient may be reversed, resulting in slightly higher EPs (≤ 5 mV) in the apex. Thus the use of the lower basal turn EP in the present work provides a reasonable indication of the extent of EP reduction by noise throughout the cochlea. Glass capillary pipettes (40–80 M Ω) filled with 0.15 M KCl were mounted on a hydraulic microdrive (Frederick Haer) and advanced until a stable positive potential was observed that did not change with increased electrode depth. The signal from the recording electrode was led to an AM Systems Model 1600 intracellular amplifier. EP changes by condition (Fig. 3) were compared within each strain by one-way analysis of variance (ANOVA) using young unexposed mice as controls. Sample sizes by strain and condition varied from six to 20.

Tissue processing for histology

At the end of recording, animals were overdosed and perfused transcardially with cold 2.0% paraformaldehyde/2.0% glutaraldehyde in 0.1 M phosphate buffer (pH 7.4). Each cochlea was rapidly isolated, immersed in the same fixative, and the stapes was immediately removed. Complete infiltration of the cochlea by fixative was ensured by making a small hole at the apex of the cochlear capsule, and gently circulating the fixative over the cochlea using a transfer pipet. After decalcification in sodium EDTA for 72 h, cochleas were post-fixed in buffered 1% osmium tetroxide, dehydrated in an ascending acetone series, and embedded in Epon. Cochleas were sectioned in the mid-modiolar plane at 4.0 μ m, then stained with toluidine blue for bright field viewing with a Nikon Optiphot™ light microscope using a calibrated grid ocular.

Morphometric analysis

Analyses were based on left cochleas, from which all recordings were obtained. Tissue sections were scored blindly. Since the mouse cochlea features just over two complete turns (Bohne et al. 2001), a typical “core” mid-modiolar section shows four profiles of the organ of Corti and lateral wall: lower base, upper base, lower apex, and upper apex (which sometimes appears only in partial profile). Quantitative assessment of cochleas focused on lateral wall, Reissner's membrane, and spiral limbus of the upper basal turn in a region expected to correspond to 10 kHz (± 0.5 octave) (Ou et al. 2000a). This was done to avoid possible artifacts associated with electrode entry in the lower basal turn. Changes we characterize in the upper basal turn were qualitatively similar elsewhere, although generally more extensive in the lower base than in the apex. Metrics obtained depended upon whether a cochlea was taken for examination 1–3 h after noise (in which case they were designed to detect changes in the appearance of cells and structures, not cell loss), or 8 weeks after noise (wherein metrics were aimed at cell loss). Examination of cochleas taken 24 h after exposure was purely qualitative. DIC images used for illustration were obtained on a Zeiss LSM 700 laser scanning confocal microscope using ZEN™ software, then further processed using CANVAS™.

Assessment of acute noise injury (1–3 h after noise)

Quantitative assessment of acute noise injury was based on 8 noise-exposed BALB mice, seven non-exposed controls, and 21 exposed N2 backcross mice. Every fifth section was analyzed through a distance of 184 μ m for a total of ten sections in each animal. Acute pathology was characterized

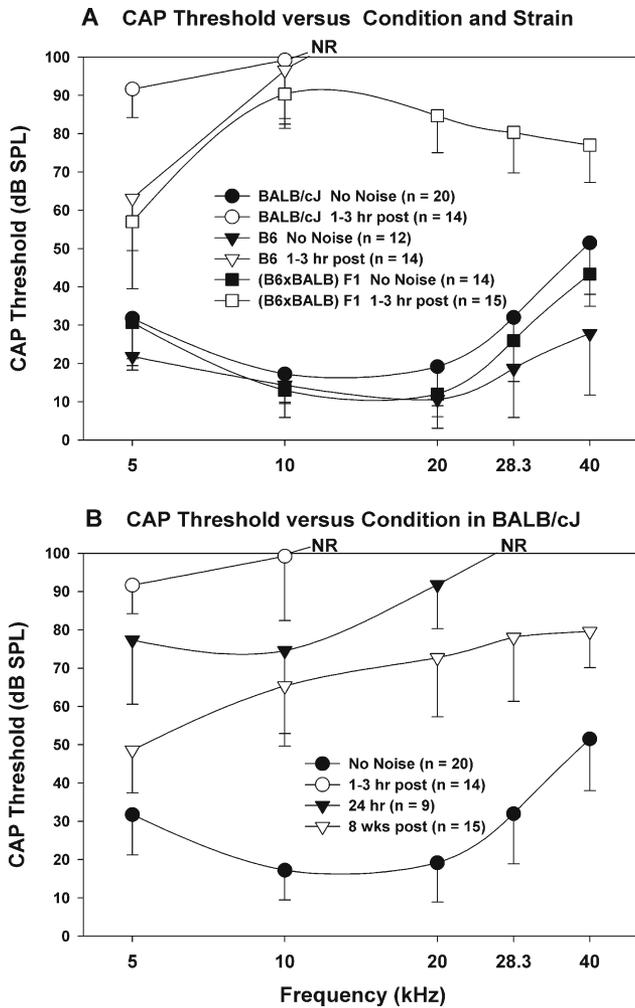


FIG. 1. **A** Mean±SD CAP thresholds for noise-exposed and unexposed control BALB, B6, and (B6×BALB) F1 mice. **B** Mean±SD CAP thresholds only for control BALB mice and BALB at various times after noise. Unexposed control and acute exposed mice (1–3 h after noise) are replotted from A to facilitate comparison. All noise exposures were 2 h, 4–45 kHz, 110 dB SPL. NR no response at highest sound level available.

non-parametrically using subjective judgments of “normal” or “abnormal” applied to stria vascularis, Reissner’s membrane, spiral ligament, and spiral limbus. Determination depended upon the clear presence of cell shrinkage, cell vacuolization, void spaces between cells, nuclear condensation, or nuclear enlargement. The cells upon which we focused were based on our previous observations in CBA/J and CBA/CaJ mice (Ohlemiller and Gagnon 2007), and included all strial cell types, types I, II, IV, and V fibrocytes in ligament, mesothelial cells of Reissner’s, and fibrocytes in the central zone of spiral limbus. The overall proportion of sections scored “normal” was compared in exposed and non-exposed BALBs by z test (Fig. 6), or calculated for each animal and tested for correlation with EP or other metrics across animals (Figs. 12 and 13).

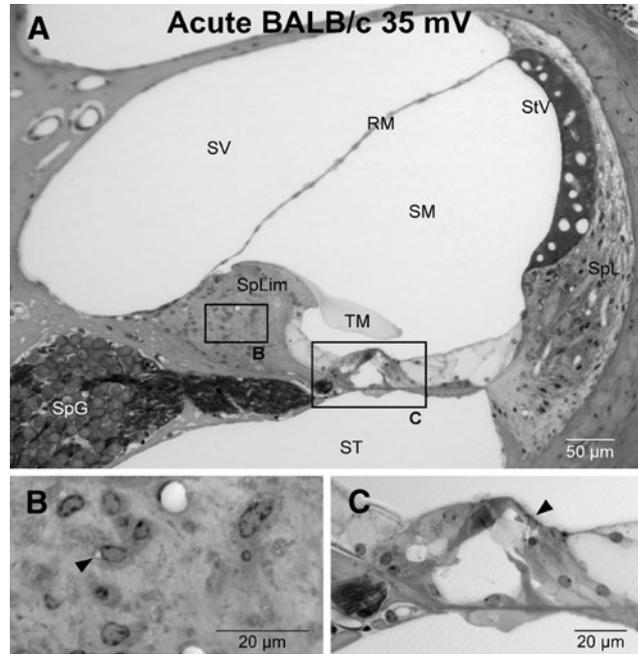


FIG. 2. **A** Typical cochlear duct of the upper basal turn in a BALB mouse 1–3 h after noise. **B** Expanded view of box centered on spiral limbus in (A). Stellate fibrocytes of limbus show subtle vacuolization (arrowhead). **C** Expanded view of organ of Corti. Pillars are bent and Nuel’s space is collapsed (arrowhead), but no breach of reticular lamina is apparent. SpL spiral ligament, StV stria vascularis, SV scala vestibuli, ST scala tympani, SM scala media, spLim spiral limbus, RM Reissner’s membrane, SpG spiral ganglion, TM tectorial membrane.

Assessment of permanent noise injury (8 week after noise)

Quantitative assessment of permanent noise injury was based on 8 BALB mice 6–7 months old at time of examination and seven age-matched non-exposed controls. Every fifth section was analyzed through a distance

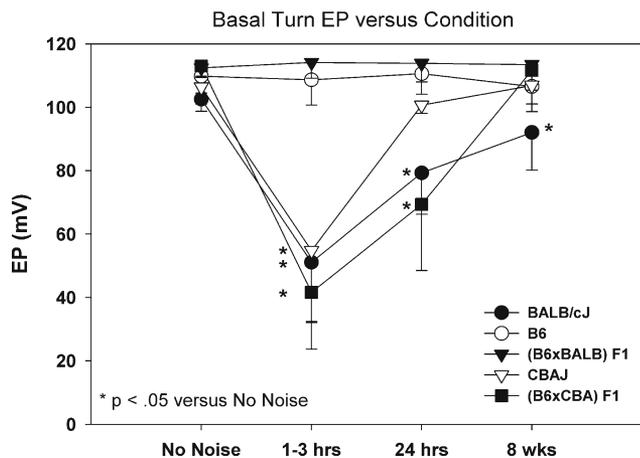


FIG. 3. Mean±SD basal turn EP in unexposed controls and at various times after noise exposure in inbred BALB, B6, and CBA/J mice, and in F1 hybrids formed from crossing BALB and CBA with B6. EP reduction by noise is dominant versus B6 in CBA; recessive in BALB. EP does not completely recover in BALBs. Asterisk Significantly different from unexposed controls of same strain by one-way ANOVA.

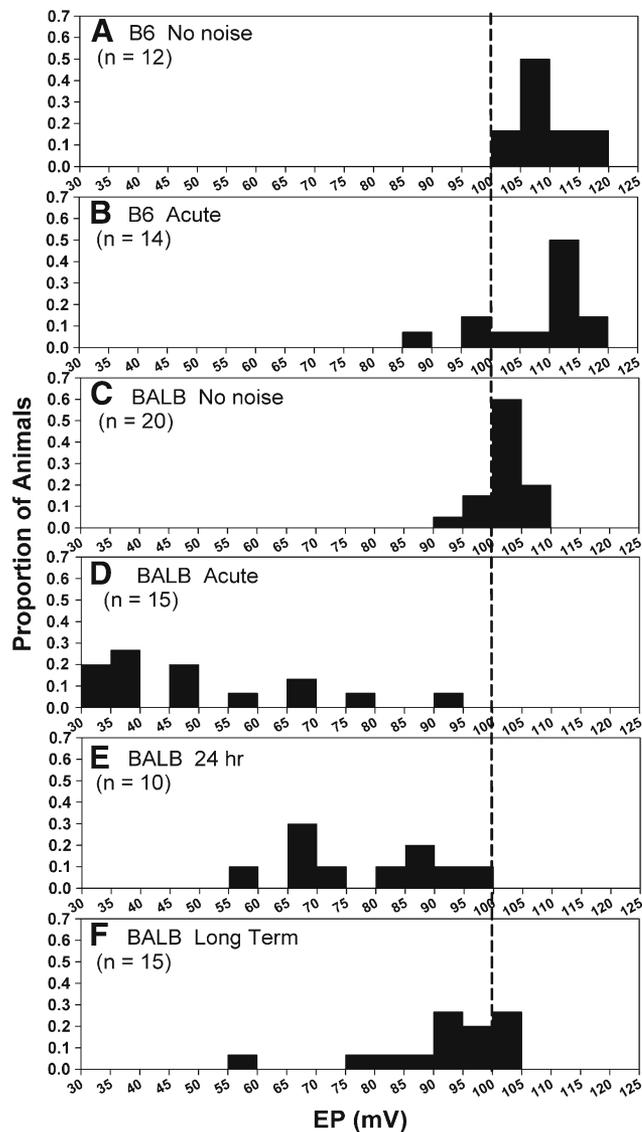


FIG. 4. A–F Distribution of basal turn EPs in B6 and BALB mice with and without noise exposure. Data are the same as those used to derive means and statistical results shown in Figure 3. BALBs are examined at various times after noise as shown. Vertical line marks 100 mV to aid comparisons. Data were derived by dividing the number of animals in each bin by sample size for each group, so that bin height indicates the proportion falling within a particular EP range.

of 184 μm for a total of ten sections per animal. Quantitative measures included stria thickness, stria marginal cell density, intermediate cell density, basal cell density, ligament thickness, density of types I, II, and IV fibrocytes in the ligament, and density of fibrocytes in adjacent spiral limbus. Only nucleated profiles were included in cell counts. Stria thickness was measured orthogonal to the midpoint. Marginal cells, intermediate cells, and basal cells were counted in an 80 μm linear segment of stria, centered at the midpoint. No attempt was made to distinguish between lower and upper level intermediate cells, a distinction recently made by Schulte and Spicer (Spicer and Schulte 2005b). Liga-

ment thickness was measured on an axis co-linear with the stria midline. Types I, II, and IV fibrocytes were counted in a 1,600 μm^2 area. These were identified based on location, an approach taken in previous studies (Hequembourg and Liberman 2001; Lang et al. 2002; Hirose and Liberman 2003). Fibrocytes in spiral limbus were also counted in a roughly centered 1,600 μm^2 area, expected to be populated principally by stellate cells (Kimura et al. 1990). For each metric, the ten estimates were averaged to yield an overall average for each animal. Parametric data from noise-exposed animals were compared with non-exposed controls of the same strain by *t* test (Fig. 9).

RESULTS

CAP thresholds in inbred and F1 mice

Noise exposure led to nearly complete loss of CAP responses above 5 kHz in both BALB and B6 mice in the acute period after noise (Fig. 1A). F1 hybrids formed from B6 and BALB seemed to gain some resistance, with most F1s exhibiting recordable responses at all frequencies. While threshold shifts are not the focus of this paper, we considered to what extent acute threshold shifts in Figure 1A may reflect the EP changes described below. As we will show, acute threshold differences between B6 and F1 mice cannot reflect EP differences, as neither of these exhibit EP reduction after noise. Note, however, that residual hearing at 5 kHz was ~ 30 dB better in B6 and F1 hybrid mice than in BALB mice, in which we demonstrate EP reduction. We previously showed that the dependence of thresholds on the EP after noise exposure in our mice is about -0.4 dB/mV at most test frequencies (Ohlemiller and Gagnon 2007; Ohlemiller 2009), compared with slopes closer to -1.0 dB/mV obtained using furosemide in cats and gerbils (Sewell 1984; Schmiedt et al. 2002). We have interpreted this to indicate that acute threshold shifts are dominated by injury to the organ of Corti. Assuming a slope much less than -1.0 dB/mV, and that the organ of Corti in the 5 kHz region sustained less injury than more basal regions, the threshold difference at 5 kHz between BALBs and the other strains is in line with the ~ 50 mV average EP reduction in these mice. By 8 weeks post-exposure, thresholds in BALBs had resolved somewhat (Fig. 1B), but remained elevated by an average ~ 50 dB at most frequencies. As we will see, in many cases part of this is due to permanent EP reduction.

Consistent with the assumption that acute threshold shifts are dominated by the organ of Corti, light microscopy revealed striking abnormalities in the organ of Corti of BALBs shortly after exposure. The example in Figure 2 shows that the organ of Corti in the upper basal turn of BALBs was distorted, featuring bending of pillars and collapse of Nuel's space (Fig. 2C). In

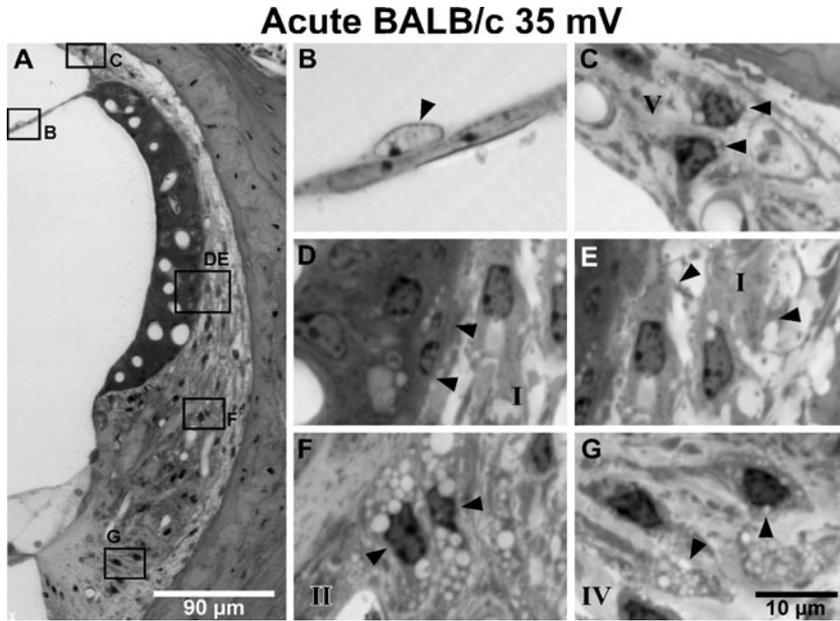


FIG. 5. A Cochlear upper basal turn lateral wall in example BALB mouse 1–3 h after noise. Animal is the same as shown in Figure 2. B Expanded view of box B in (A) showing enlarged pale nucleus of mesothelial cell of Reissner's membrane (arrowhead). C Expanded view of box C in (A) showing vacuolated type V fibrocytes (arrowheads). D–E Expanded view of boxes D and E in (A) showing vacuolated basal cells and possibly intermediate cells in stria with adjacent shrunken type I fibrocytes in spiral ligament (arrowheads). Shrinkage of fibrocytes is attended by increased clear space in ligament. F Expanded view of box F in (A) showing vacuolated type II fibrocytes (arrowheads). G Expanded view of box G in (A) showing vacuolated type IV fibrocytes (arrowheads). Roman numerals in (C–G) denote major constituent fibrocyte types.

no case, however, did the reticular lamina appear ruptured, nor was there any other sign of breaching of the boundaries of scala media. In addition, spiral limbus was significantly more likely to show vacuolization of stellate fibrocytes than in unexposed controls (Figs. 2B and 6).

Effects of noise on EP in inbreds and F1s

Figure 3 compares the average EP in BALBs and comparison groups in controls, and at various times after noise. The EP in BALBs was reduced by 50–60 mV in the hours after exposure. The EP remained significantly depressed 24 h later, and still remained signifi-

cantly depressed by an average ~10 mV at 8 weeks post-exposure. B6 mice showed no EP reduction at any time. Like CBAs, F1s formed from B6 and CBA showed EP reduction that recovered completely by 8 weeks. By contrast, F1s formed from B6 and BALB showed no EP reduction by noise at any time. The fact that these F1 mice do not display an intermediate phenotype suggests that all EP susceptibility alleles in BALBs act in a simple recessive manner, and may be few in number.

Figure 4 re-analyzes data from Figure 3, showing the distribution of EPs in BALBs at various times after noise, and comparing these with B6 mice. In each graph, each bin represents the proportion of animals having an EP within a particular 5 mV range. Slightly different modal values in unexposed B6 and BALB mice (compare Fig. 4A, C) are in keeping with our previous observation (Ohlemiller et al. 2006) that young 'normal' BALBs have an EP that is on average ~10 mV lower than in B6. In the hours after noise, nearly all BALBs showed an EP below 80 mV, while B6 mice showed no average change. By 24 h later, the EP in some BALBs had returned to near-normal (Fig. 4E). However, even 8 weeks after noise the EP remained significantly depressed on average as a result of marked leftward skewing of the EP distribution (Figs. 3 and 4F).

Morphological correlates of acute EP changes

We previously showed that several lateral wall cell types in the cochlear upper basal turn of CBA mice show acute pathology that correlates with EP reduction within hours after noise (Ohlemiller and Gagnon 2007; Ohlemiller et al. 2010b). This pathology was manifested not as cell loss at this early time point, but rather in the form of cell vacuolization, shrinkage,

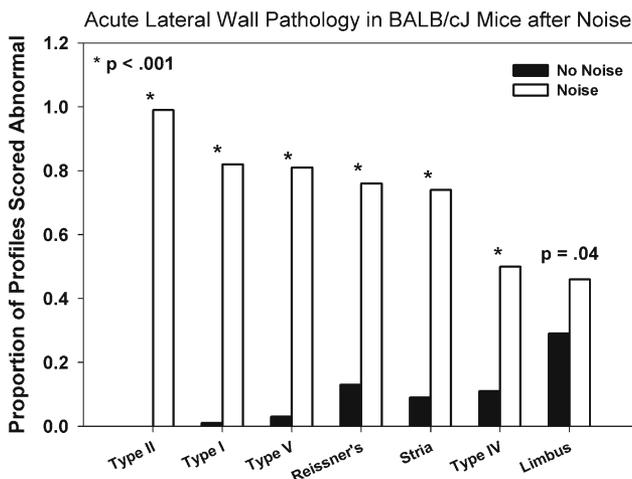


FIG. 6. Quantitative analysis of acute (1–3 h post) noise-related pathology of lateral wall and spiral limbus in noise-exposed and control BALB mice. Sections were blindly scored "normal" or "abnormal" for each cell type or structure, and section totals were combined for each experimental group. *P* values indicate *z* test results.

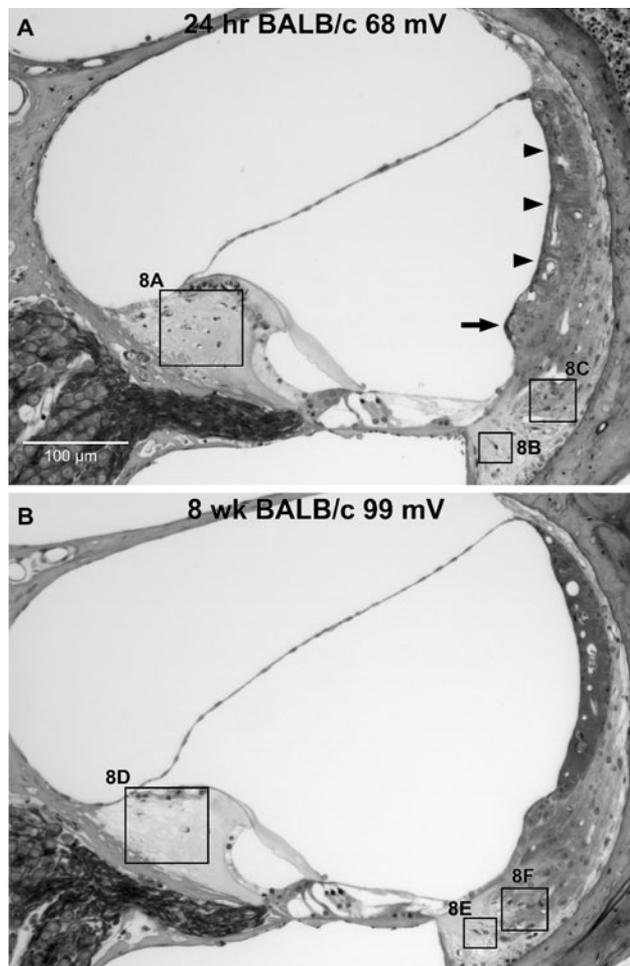


FIG. 7. **A** Example cochlear upper basal turn of BALB mouse taken for examination 24 h after noise exposure. Stria is swollen (*arrowheads*) and epithelial cells of spiral prominence are darkened (*arrow*). **B** Example cochlear upper basal turn of BALB mouse taken for examination 8 weeks after noise exposure. EPs are as shown. Boxes denoted 8A–8F refer to expanded views in Figure 8.

or nuclear pyknosis. BALBs showed similar effects in virtually all the same cells as CBAs, as shown by example in Figure 5, and quantitatively in Figure 6 (Note that we did not quantify as many cell types in the earlier CBA study.). The acute effects of noise were apparent in several structures, including Reissner's membrane, stria vascularis, spiral ligament, and spiral limbus. Noise-related changes within Reissner's membrane, stria, and ligament were highly distinctive and not easily confused with processing artifacts, and included enlargement and paling of the nucleus of mesothelial cells on Reissner's upper surface (Fig. 5B), vacuolization of types II, IV, and V fibrocytes (Fig. 5C, F, G), and shrinkage of type I fibrocytes (Fig. 5E). The stria itself showed vacuoles that were usually confined to the basal cell layer, but occasionally extended into the middle stria layers (Fig. 5D). Strial capillaries rarely appeared distended, collapsed, or otherwise abnormal. At the light microscope level,

acute stria changes appeared mostly intracellular, and not as edema.

Judged quantitatively, differences versus non-exposed controls in the percent of sections scored abnormal after noise were highly significant (Fig. 6). The cells least reliably distinguishable in noise versus control animals were type IV fibrocytes, and cells of spiral limbus. Type IV's were scored abnormal in controls in ~10% of sections, and scored abnormal in exposed animals in ~50% of sections, which was nevertheless a significant difference by *z* test ($p < .001$). The relatively high percentage of type IV's scored abnormal may in part reflect an attempt to apply inclusive criteria. Upon re-inspection, type IV fibrocytes labeled abnormal in controls tended to be labeled based on their pyknotic nuclei, while those in noise-exposed animals tended to show vacuoles like those shown in Figure 5G. Cells of spiral limbus were scored abnormal in ~30% of controls sections and ~55% of exposed animals, a smaller difference that was nevertheless significant ($p = .04$). The frequent abnormal appearance of the limbus included vacuolization of stellate cells, and pyknotic nuclei of both stellate cells and interdental cells. It is not clear whether abnormal features of ligament and limbus in nominally normal animals reflect sub-optimal preservation, or perhaps ongoing loss and turnover of these cells.

Consistent with previous reports (Duvall et al. 1974; Ide and Morimitsu 1990; Wang et al. 2002; Hirose and Liberman 2003), by 24 h after noise exposure the manner of abnormal appearance of the stria changed from vacuolization of some cells to swelling of the intrastrial space, imparting a swollen profile to the stria (arrowheads in Fig. 7A). By this time, signs of fibrocyte death began to appear, particularly among type II and IV fibrocytes of the ligament and stellate fibrocytes of spiral limbus (Fig. 8A–C). More so than we observed in CBAs, BALBs also tended toward darkening of the cells of the spiral prominence epithelium at this time (see arrow in Fig. 7A).

Permanent effects of noise in inbreds

We previously showed that most of the same cells and structures exhibiting acute effects of noise in CBA mice also showed changes 8 weeks later (Ohlemiller and Gagnon 2007). As determined by morphometry of the upper basal turn, all the lateral wall and limbus cell types noted to be abnormal acutely after noise in CBAs, including type I and II fibrocytes and stria basal cells, were significantly reduced in number at 8 weeks. In addition, stria capillaries were reduced in number in CBAs, and both stria and ligament became significantly thinner. Given that the EP completely recovers in CBAs, but shows incomplete recovery in BALBs, we anticipated greater cell loss and permanent injury in BALBs. This

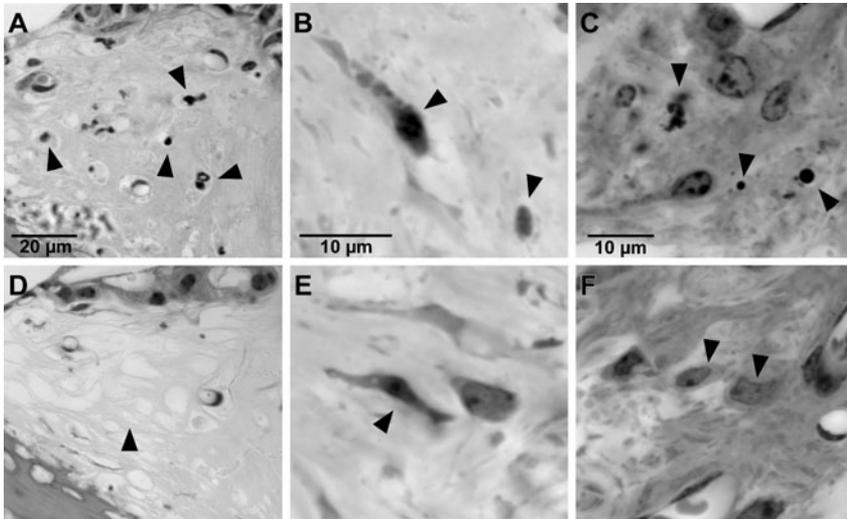


FIG. 8. Expanded views of boxed regions in Figure 7. **A–C** At 24 h post-exposure, pyknotic nuclei and condensed cells of spiral limbus and in regions of ligament dominated by type IV fibrocytes and type II fibrocytes, respectively, indicate dying cells (*arrowheads*). **D–F** By 8 weeks post-exposure, stellate fibrocytes of limbus are entirely missing in upper base and lower apex (*arrowhead* in **(D)**). Type IV fibrocytes are reduced in number. *Arrowhead* in **(E)** shows dying type IV. Type II fibrocytes (**F**, *arrowheads*) appear generally normal.

was not the case, however. A more extensive inventory of cell loss and other structural changes in the upper base 8 weeks after exposure in BALBs revealed significant loss of only type IV fibrocytes and stellate fibrocytes of limbus (Figs. 7B, 8D–F, and 9A). While the stria showed significant thinning (Fig. 9B), ligament showed no difference. Acute pathology of the epithelium of spiral prominence frequently observed in BALBs did not lead to clear degeneration of epithelial cells at 8 weeks. A thin layer of cells covering the prominence was seen in all cases.

Inheritance pattern of EP and lateral wall injury in N2 backcross mice

As an initial approach to the genetics of the different EP phenotypes in BALB and B6 mice, we bred and noise-exposed (B6×BALB) F1 hybrids and (F1×BALB) N2 backcross mice. Figure 10 compares the distribution of EPs measured acutely after noise in both models. To facilitate comparison, data from the unexposed inbred lines have been recapitulated (Fig. 10A, B). The F1 data suggest a hybrid advantage in both unexposed and exposed mice (Fig. 10C, D). Both show EPs that appear slightly higher on average than in unexposed, although this trend was not significant by one-way ANOVA. EPs from unexposed N2 mice were surprisingly broadly distributed, and included a mode at distinctly lower EPs than seen in either of the parent strains (compare Fig. 10A, B, E). These N2s may be homozygous for BALB alleles responsible for the slightly low “normal” EP in BALB inbreds. EPs in noise-exposed N2s were highly skewed toward lower values (Fig. 10F), with one quarter (14/56) of the mice showing EPs below 80 mV. This is consistent with a requirement of homozygosity for BALB alleles at two or more loci for the EP to be reduced by noise.

Histologic correlates of acute EP reduction in N2 mice

In N2 mice formed from B6 and CBA, we previously demonstrated strong correlations between metrics for acute pathology of stria, spiral ligament, and Reissner’s membrane versus the EP (Ohlemiller and Gagnon 2007; Ohlemiller et al. 2010b) (Table 1). We therefore conducted similar analyses in noise-exposed N2s formed from B6 and BALB, selecting mice with EPs among the lowest recorded ($n=11$), and the highest recorded ($n=10$). Unlike B6/CBA N2 mice, two distinct patterns were noted among B6/BALB N2 mice with a low EP, based on the appearance of stria vascularis and type I fibrocytes. Some mice with a low EP featured a normal appearing stria with abnormal type I’s (Fig. 11B, D). Other mice with a low EP combined a clearly abnormal stria with normal appearing type I’s (Fig. 11C, F, G). Mice showing a low EP reliably exhibited abnormal appearance of Reissner’s membrane (example not shown) and type II fibrocytes (Fig. 11B, C, E, H).

Trends described above could be demonstrated quantitatively, as shown in Figure 12. Among all metrics, the appearance of Reissner’s membrane and type II fibrocytes were most strongly correlated with EP ($R^2 \geq .70$) (Fig. 12A, B). Abnormal appearance of stria, type V fibrocytes, and type I fibrocytes were progressively less reliable predictors of a low EP (Fig. 11C–E), although correlations were still significant. The appearance of type IV fibrocytes (Fig. 11F) and spiral limbus (not shown) were completely uncorrelated with EP. The very different relations between the predictive value for the EP of the appearance of stria vascularis and type I fibrocytes in CBA- versus BALB-derived N2 mice are highlighted in Table 1, which compares the coefficients of determination of their respective

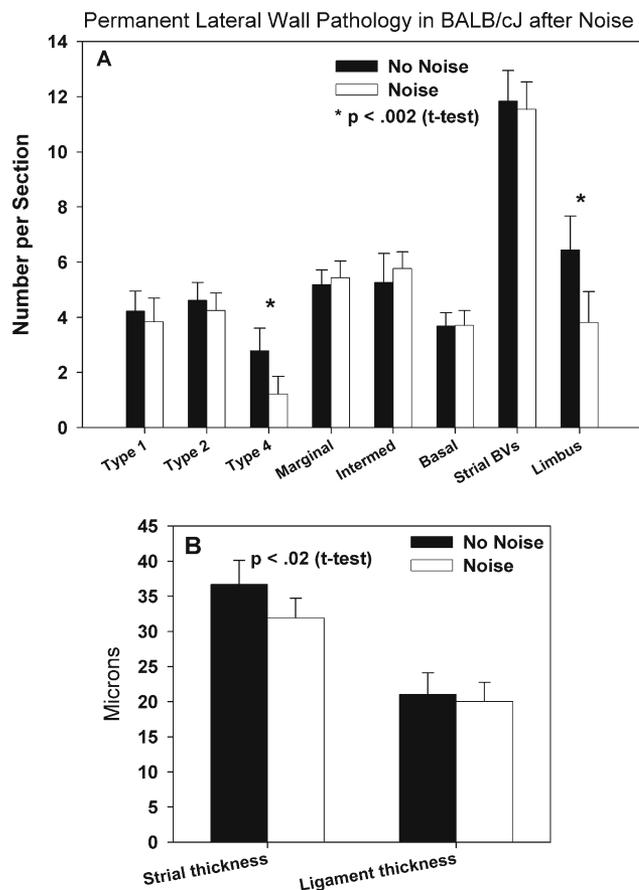


FIG. 9. Quantitative analysis of permanent noise-related pathology (8-week post-exposure) in cochlear upper basal turn spiral limbus and lateral wall of control and exposed BALB mice. **A** Among metrics for strial and ligament cell types, as well as strial capillaries (blood vessel density (BV_s)), significant differences were only found for type IV fibrocytes and stellate fibrocytes of limbus. **B** Significant thickness changes were found for stria, but not ligament. P values denote results of two-tailed *t* test.

linear regressions. Neither strial nor type I fibrocyte pathology were as strongly correlated with EP in B6/BALB N2s as in B6/CBA N2 mice. Accordingly, the relation between strial and type I fibrocyte pathology is quite different in the two models. As Figure 13 shows, these are strongly correlated in B6/CBA N2s, but completely uncorrelated in B6/BALB N2s. From these data we conclude that noise-related EP reduction in BALBs can arise from somewhat independent cascades within stria and ligament. These may reflect the action of different genes.

DISCUSSION

Until recently the role of EP reduction in acute and permanent NIHL has been largely undefined. When traumatic noise breaches the boundaries of scala media, the EP almost certainly decreases, and may or may not

recover (Ward and Duvall 1971; Johnsson and Hawkins 1972; Duvall et al. 1974; Santi and Duvall 1978; Ulehlova 1983; Ide and Morimitsu 1990; Ahmad et al. 2003). For less traumatic noise insults where endolymphatic boundaries remain intact, the expectation has been that the EP is unaffected or only transiently affected, and does not impact the degree of permanent NIHL. Our current and recent work builds upon work by Hirose, Liberman, and colleagues (Wang et al. 2002; Hirose and Liberman

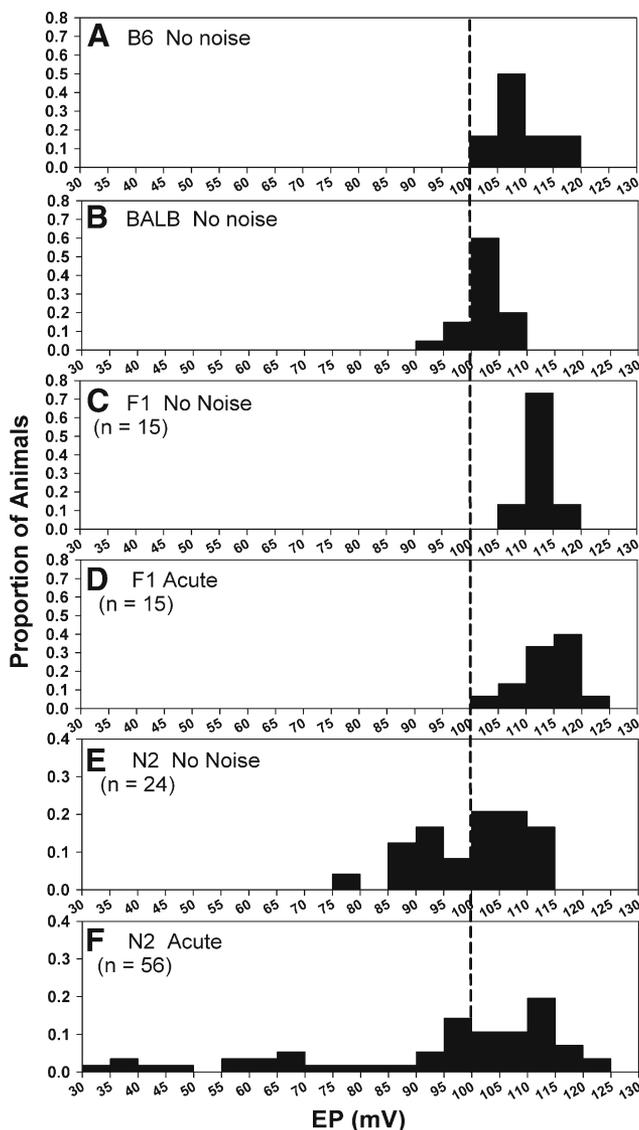


FIG. 10. A–B Distribution of basal turn EPs in B6 and BALB mice without noise exposure (reproduced from Figure 4 to aid comparison). C–D Distribution of EPs with and without noise in (B6 × BALB) F1 hybrid mice. E–F Distribution of EPs in (F1 × BALB) N2 backcross mice with and without noise. Following noise, 25% (14/56) of N2 mice showed EPs below 80 mV. Note different y-axis range in (E) and (F) due to greater scatter. Vertical line marks 100 mV to facilitate comparisons. As in Figure 4, data were derived by dividing the number of animals in each bin by sample size for each group, so that bin height indicates the proportion falling within a particular EP range.

TABLE 1

Coefficients of determination (R^2) for EP versus lateral wall injury metrics in [(B6×CBA)×B6] N2 and [(B6×BALB)×BALB] N2 mice

EP versus	B6/CBA N2		B6/BALB N2	
	R^2	P	R^2	P
Reissner's pathology	0.9 ^a	<.001	0.72	<.001
Strial pathology	0.78 ^b	<.001	0.55	<.001
Type II pathology	0.69 ^b	<.001	0.70	<.001
Type I pathology	0.57 ^b	<.001	0.27	0.013

^aFrom Ohlemiller et al. 2010b

^bFrom Ohlemiller and Gagnon 2007

2003; Hirose et al. 2005) by demonstrating that (1) EP reduction by noise can occur in instances where the boundaries of scala media are maintained; (2) Whether EP reduction occurs depends on genetically modifiable

factors that are probably intrinsic to the lateral wall; (3) EP reduction may reflect independent cascades within stria vascularis and the spiral ligament; and (4) Depending on the genes and alleles involved, EP reduction may not be completely reversible. For our particular noise exposure the degree of permanent reduction averaged a modest ~10 mV in BALB mice. Rather than supporting any particular amount of EP reduction or any required exposure condition, we regard the noise phenotype of BALBs simply as an indication that permanent EP reduction by noise is neither special nor atypical. Only one noise condition and relatively little of the extant genetic diversity of mice had to be "mined" to demonstrate permanent EP reduction. Thus we suppose that alleles favoring a wide range of lateral wall responses to noise will be found across animal and human populations, and that there exists no single

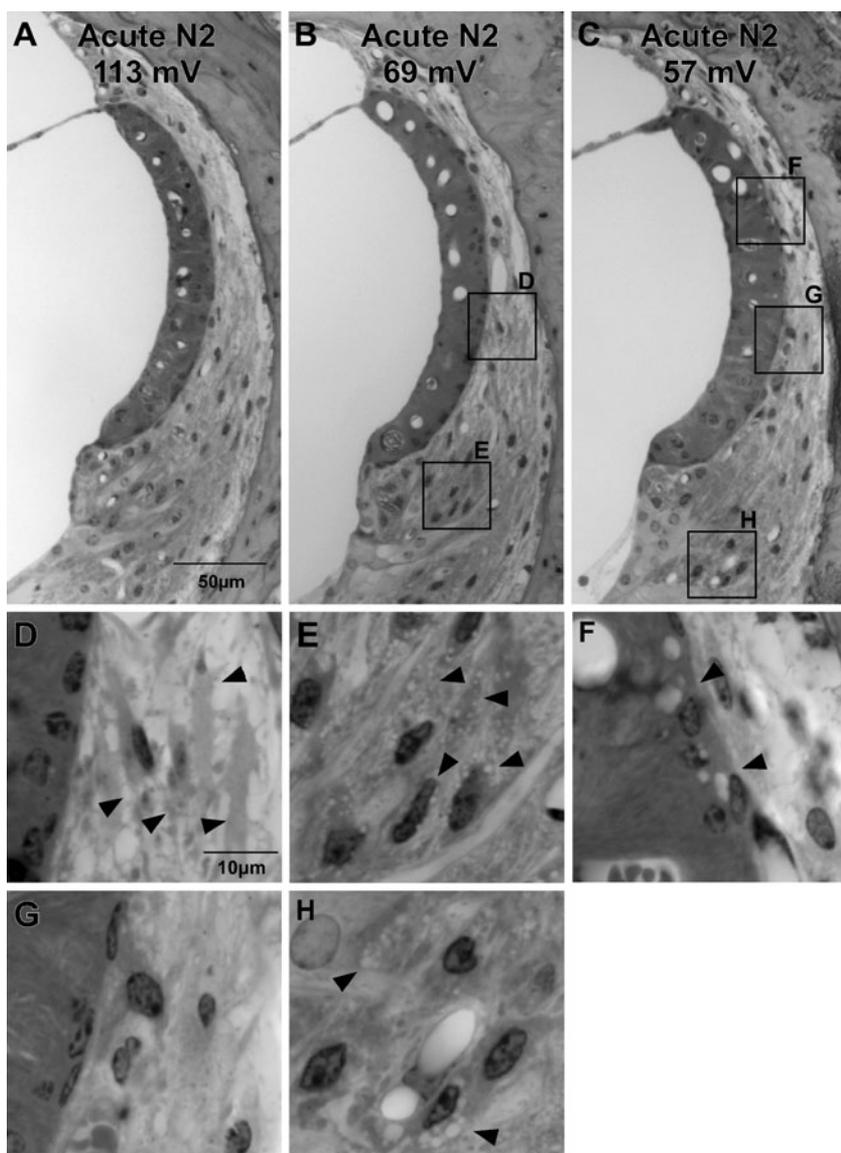


FIG. 11. Examples of the three major patterns of cellular appearance observed in the cochlear upper basal turn 1–3 h after noise in B6/BALB N2 back-cross mice. EPs are shown for each animal. **A** Normal EP attended by minimal pathology, as detected by light microscope. **B** Mouse with reduced EP combining minimal strial pathology with clear pathology of type I fibrocytes (expanded in **D**), arrowheads) and type II fibrocytes (expanded in **E**), arrowheads). **C** Mouse combining clear strial pathology (expanded in **F**), arrowheads) with pathology of type II fibrocytes (expanded in **H**), arrowheads), but showing minimal pathology of type I fibrocytes (expanded in **G**).

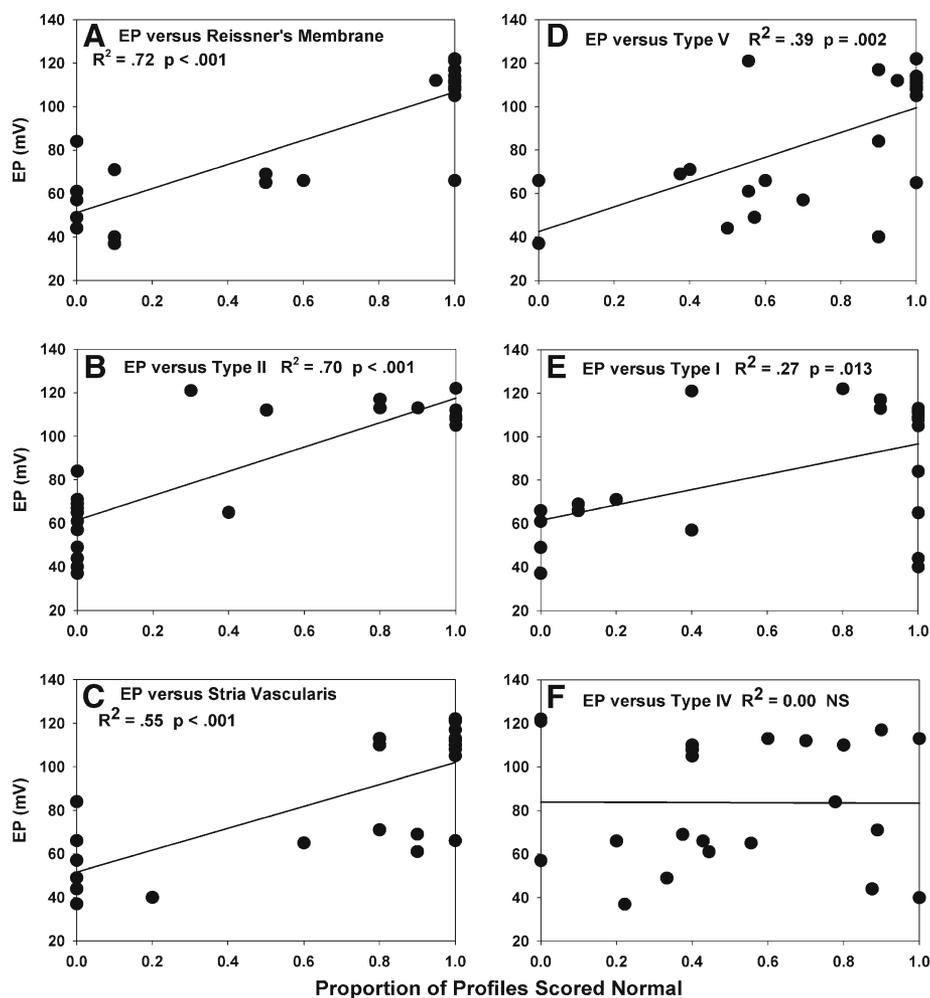


FIG. 12. A–F Correlation between basal turn EP and pathology of specific cells and structures in the upper basal turn of B6/BALB N2 backcross mice, observed 1–3 h after noise. The condition of Reissner's membrane and type II fibrocytes of ligament showed the strongest correlation with EP (A, B), followed by progressively weaker correlation between EP and the appearance of the stria (C), type V fibrocytes (D), and type I fibrocytes (E). The appearance of type IV fibrocytes (F) and spiral limbus (not shown) was uncorrelated with EP.

cellular pattern of noise-related cochlear pathology in mammals.

Anatomic correlates of acute EP reduction

Our acute observations in BALB inbred mice point to a broad range of affected non-sensory cell types and structures, including strial basal cells, and most constituent cells of spiral ligament and limbus. We interpreted a similar pattern in CBA mice as indicating that all the affected cells participate in the same pathologic cascade, and considered which cell(s) are likely to express the product encoded by the *Nirep* QTL (Ohlemiller et al. 2010b). The accepted broad conceptual framework for operation of the lateral wall is that of return path for K^+ that is “recycled” after passing through the organ of Corti (Spicer et al. 1996; Wangemann 2002). The concentration gradients driving K^+ movement are largely established by ATPases in type II fibrocytes and strial marginal cells. If the most “downstream” point—that is, the stria—were to become functionally impaired, then K^+ could build up

in ligament. Assuming K^+ accumulates inside of type II fibrocytes but outside of type I fibrocytes, the very different appearance of these cells (vacuolation of type II, shrinkage of type I) might be explained. Further, accumulation of K^+ and other ions outside type I fibrocytes could occur if the normally ion-tight boundary of the lateral stria were rendered porous by noise. That boundary is composed of tight junctions between basal cells, the most obviously affected strial cell type in our mice. All these events could thus be linked in CBA mice, with the probable site of *Nirep* expression lying within the stria. Our finding of somewhat independent pathology of stria and type I's in B6/BALB N2 mice seems less compatible with a ‘leaky stria’ scenario. In both BALB and CBA, however, the condition of both type II fibrocytes and Reissner's membrane was highly correlated with the EP, suggesting these spatially separated cells participate in a common affected process.

To extract strain differences from broad patterns of change, we deliberately focused on changes discernable at the light microscope level. Thus our observation that basal cells appeared to be the most affected strial cell type in BALBs is not meant to imply

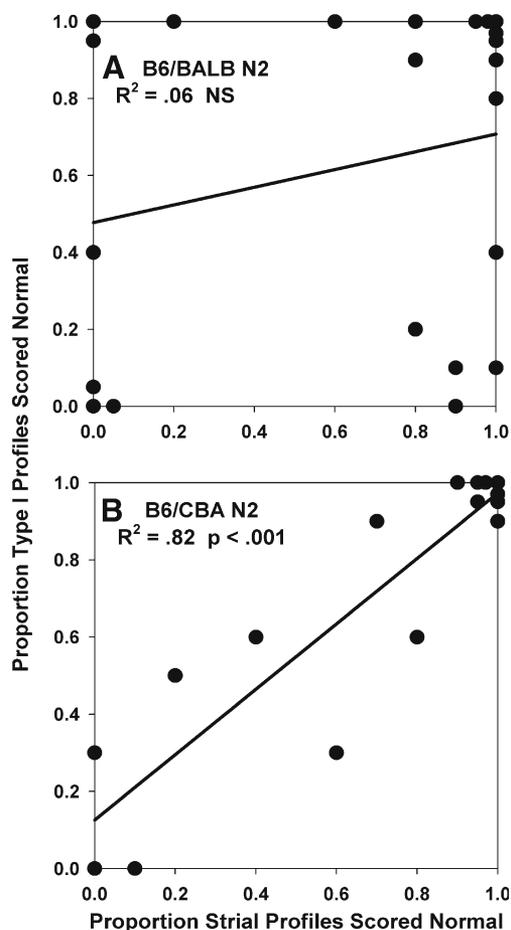


FIG. 13. Direct comparison the correlation between acute noise-related pathology of stria vascularis and type I fibrocytes of spiral ligament in B6/BALB N2 mice (A) and B6/CBA N2 mice (B). These were highly correlated in B6/CBA N2s, but completely uncorrelated in B6/BALB N2s.

that intermediate and marginal cells were unaffected by noise. The extent of intermediate and marginal cell involvement clearly depends on exposure conditions (Hirose and Liberman 2003). Marginal cells express several components key to the generation of the EP (Hibino and Kurachi 2006; Wangemann 2006), and appear to be metabolically labile (e.g., Spicer and Schulte 2005a; Ohlemiller et al. 2009). They are also the principal strial site of expression of the $\text{Na}^+/\text{K}^+/\text{Cl}^-$ exchanger (*Slc12a2*), a strong candidate for *Nirep* (Ohlemiller et al. 2010b).

The B6/BALB N2 data suggest that acute pathology of type IV fibrocytes and spiral limbus cells are indirectly related or unrelated to EP reduction, since changes in these were poorly correlated with EP (Fig. 12). Strictly noise-related pathology was also hardest to show in these cells (Fig. 6), potentially obscuring the true relationship. It may be the case that BALBs harbor alleles that promote noise injury in type IV and limbus fibrocytes independent of EP change and its

genetics. While we did not quantify type IV pathology in CBAs, we and others have identified type IVs as a target of noise in both CBA and B6 mice (Hirose et al. 2005; Ohlemiller and Gagnon 2007). Permanent limbus pathology, however, appears to segregate with acute EP vulnerability, being readily observed in both CBA and BALB, but less so in B6 (Ohlemiller and Gagnon 2007). We could not use the N2 mice to try to separate permanent limbus pathology from EP vulnerability, since there would be no way of knowing whether mice exhibiting clear loss of limbus fibrocytes 8 weeks after noise would have shown acute EP reduction. It presently remains unclear whether spiral limbus pathology can be viewed as part of the cascade that reduces the EP in BALB and CBA mice, and what this may reveal about mechanisms.

Anatomic correlates of permanent EP reduction

Given the overall match between acute and permanent pathology we observed in CBA mice (Ohlemiller and Gagnon 2007; Ohlemiller et al. 2010b), which do not show permanent EP reduction from our noise exposure, we expected even more prominent permanent changes in the cochlear lateral wall of BALB mice. Instead, we were surprised to observe only modest changes restricted to type IV fibrocytes, spiral limbus, and strial thickness (Fig. 9). Light microscopy alone is not adequate to explain this discrepancy, and ultrastructural analysis or examination of major lateral wall protein expression (e.g., Na^+/K^+ -ATPase, $\text{Na}^+/\text{K}^+/\text{Cl}^-$ co-transporter, KCNJ10) (Hibino and Kurachi 2006; Wangemann 2006) maybe required. Because it was easy to find dying type II fibrocytes in spiral ligament 24 h after noise (Fig. 8), it was particularly surprising that no permanent loss of these cells was detected. Renewal of cells in spiral ligament has been demonstrated in mice and other models (Lang et al. 2003, 2006; Yamasoba et al. 2003), and it maybe that renewal processes are more robust in BALBs than in CBAs.

We previously showed that by 19 months of age BALB/c mice exhibit age-associated EP reduction whose major anatomic correlates are marginal cell loss and thinning of spiral ligament (Ohlemiller et al. 2006; Ohlemiller 2009). Although it is not clear which strial cell changes underlie strial thinning after noise, neither marginal cell loss nor thinning of the ligament was clearly exacerbated (Fig. 9). Thus there appears no obvious overlap between the targets of noise and aging in the BALB lateral wall, at least at 6 months of age. It remains to be seen whether the typical aging trajectory of the BALB lateral wall can be altered by earlier noise exposure. Permanent noise injury to the lateral wall may exert effects on hearing apart from any impact on the EP, of course.

It is becoming increasingly clear that the spiral ligament does more than supply K^+ to the stria. It also may mediate passage of metabolites from strial and ligament capillaries into the organ of Corti (Chang et al. 2008; Ohlemiller 2008), or otherwise participate in protective or injury cascades that affect the organ of Corti (Sautter et al. 2006; Shi and Nuttall 2007; Adams 2009).

Genetic basis of “normal” and noise-reduced EP in BALB

The noise phenotype of (B6×BALB) F1 mice and the distribution of EPs in acutely exposed B6/BALB N2 mice are consistent with a small number of recessive acting QTLs. Apparently, at least two loci must operate in combination, since only about one quarter of the N2s show acute EP reduction by noise. Given the evidence for independent processes in stria and ligament (Fig. 13), it is possible that two genes are expressed principally in ligament and stria, respectively. One of these could be *Nirx1*, but if so, seems likely to be a different allele than that carried by CBAs. The $Na^+/K^+/Cl^-$ co-transporter expressed by strial marginal cells lies within the ~30 cM 95% confidence for *Nirx1*. There are some similarities between the acute pathology we find in BALB and CBA and the effects of metabolic poisons (Hoya et al. 2004; Okamoto et al. 2005; Yamasoba et al. 2006) and locally applied furosemide (Schmiedt et al. 2002), suggesting that *Nirx1* encodes the co-transporter, or some factor involved in metabolism.

Since the literature to our knowledge contains no reports of naturally occurring alleles that subtly influence the EP, some novel features of the EP distributions in Figure 10 merit emphasis. The distribution of EPs in both exposed and non-exposed F1 and N2 mice is consistent with one or more dominant-acting alleles in B6 that *increase* the EP versus ‘normal’ BALBs. As evidence for this, in Figure 10C–F the upper edge of each distribution appears somewhat right-shifted (versus unexposed BALBs) for both exposed and unexposed F1 and N2 mice. Intriguingly, the EP distribution for unexposed N2s (Fig. 10E) also includes a left-shifted mode that may indicate the influence of a recessive BALB allele that acts to reduce the EP versus B6 (Ohlemiller et al. 2006; Ohlemiller 2009). Mapping and identification of these suggested QTLs may provide insights into how the EP is normally set for optimal hearing.

ACKNOWLEDGMENTS

Supported by NIH R01 DC03454 and DC08321 (K.K. Ohlemiller), P30 DC04665 (R. Chole), and Washington University Med. School Dept. of Otolaryngology.

REFERENCES

- ADAMS JC (2009) Immunocytochemical traits of type IV fibrocytes and their possible relations to cochlear function and pathology. *J Assoc Res Otolaryngol* 10:369–382
- AHMAD M, BOHNE BA, HARDING GW (2003) An in vivo tracer study of noise-induced damage to the reticular lamina. *Hear Res* 175:82–100
- BEAGLEY HA (1965) Acoustic trauma in the guinea pig. I. Electrophysiology and histology. *Acta Otolaryngol* 60:437–451
- BOHNE BA, HARDING GW, OU HC (2001) Preparation and evaluation of the mouse temporal bone. In: Willott JF (ed) *Handbook of mouse auditory research*. CRC Press, Boca Raton, FL, pp 171–187
- CHANG Q, TANG W, AHMAD S, ZHOU B, LIN X (2008) Gap junction mediated intercellular metabolite transfer in the cochlea in compromised in connexin 30 null mice. *PLoS ONE* 3:e4088
- COVELL WP (1953) Histologic changes in the organ of Corti with intense sound. *J Comp Neurol* 99:43–59
- DUVALL AJ, WARD WD, LAUHALA KE (1974) Stria ultrastructure and vessel transport in acoustic trauma. *Ann Otol* 83:498–514
- HAMERNIK RP, PATTERSON JH, TURRENTINE GA, AHROON WA (1989) The quantitative relation between sensory cell loss and hearing thresholds. *Hear Res* 38:199–212
- HARDING GW, BAGGOT PJ, BOHNE BA (1992) Height changes in the organ of Corti following noise exposure. *Hear Res* 63:26–36
- HEQUEMBOURG S, LIBERMAN MC (2001) Spiral ligament pathology: a major aspect of age-related cochlear degeneration in C57BL/6 mice. *J Assoc Res Otolaryngol* 2:118–129
- HIBINO H, KURACHI Y (2006) Molecular and physiological bases of the K^+ circulation in the mammalian inner ear. *Physiology* 21:336–344
- HIROSE K, LIBERMAN MC (2003) Lateral wall histopathology and endocochlear potential in the noise-damaged mouse cochlea. *J Assoc Res Otolaryngol* 4:339–352
- HIROSE K, DISCOLO CM, KEASLER JR, RANSOHOFF R (2005) Mononuclear phagocytes migrate into the murine cochlea after acoustic trauma. *J Comp Neurol* 489:180–194
- HOYA N, OKAMOTO Y, KAMIYA K, FUJII M, MATSUNAGA T (2004) A novel animal model of acute cochlear mitochondrial dysfunction. *NeuroReport* 15:1597–1600
- IDE M, MORIMITSU T (1990) Long term effects of intense sound on endocochlear DC potential. *Auris Nasus Larynx* 17:1–10
- JOHNSON L-G, HAWKINS JE (1972) Strial atrophy in clinical and experimental deafness. *Laryngoscope* 82:1105–1125
- JOHNSON L-G, HAWKINS JE (1976) Degeneration patterns in human ears exposed to noise. *Ann Otol* 85:725–739
- KIMURA RS, NYE CL, SOUTHWARD RE (1990) Normal and pathologic features of the limbus spiralis and its functional significance. *Am J Otolaryngol* 11:99–111
- KUJAWA SG, LIBERMAN MC (2009) Adding insult to injury: cochlear nerve degeneration after ‘temporary’ noise-induced hearing loss. *J Neurosci* 29:14077–14085
- LANG H, SCHULTE BA, SCHMIEDT RA (2002) Endocochlear potentials and compound action potential recovery: functions in the C57BL/6J mouse. *Hear Res* 172:118–126
- LANG H, SCHULTE BA, SCHMIEDT RA (2003) Effects of chronic furosemide treatment and age on cell division in the adult gerbil inner ear. *J Assoc Res Otolaryngol* 4:164–175
- LANG H, EBIHARA Y, SCHMIEDT RA, MINAMIGUCHI H, ZHOU D, SMYTHE NM, LIU L, OGAWA M, SCHULTE BA (2006) Contribution of bone marrow hematopoietic stem cells to adult mouse inner ear: mesenchymal cells and fibrocytes. *J Comp Neurol* 496:187–201
- LIBERMAN MC, DODDS LW (1984) Single neuron labeling and chronic cochlear pathology. III. Stereocilia damage and alterations of threshold tuning curves. *Hear Res* 16:55–74
- LIBERMAN MC, KIANG N-YS (1978) Acoustic trauma in cats: cochlear pathology and auditory nerve activity. *Acta Otolaryngol* 358:1–63

- LIBERMAN MC, MULROY MJ (1982) Acute and chronic effects of acoustic trauma: cochlear pathology and auditory nerve pathophysiology. In: Hamernik RP, Henderson D, Salvi R (eds) *New perspectives on noise-induced hearing loss*. Raven Press, New York, pp 105–135
- NORDMANN AS, BOHNE BA, HARDING GW (2000) Histopathological differences between temporary and permanent threshold shift. *Hear Res* 139:13–30
- OHLEMILLER KK (2008) Recent findings and emerging questions in cochlear noise injury. *Hear Res* 245:5–17
- OHLEMILLER KK (2009) Mechanisms and genes in human strial presbycusis from animal models. *Brain Res* 1277:70–83
- OHLEMILLER KK, GAGNON PM (2007) Genetic dependence of cochlear cells and structures injured by noise. *Hear Res* 224:34–50
- OHLEMILLER KK, LETT JM, GAGNON PM (2006) Cellular correlates of age-related endocochlear potential reduction in a mouse model. *Hear Res* 220:10–26
- OHLEMILLER KK, RICE MR, LETT JM, GAGNON PM (2009) Absence of strial melanin coincides with age associated marginal cell loss and endocochlear potential decline. *Hear Res* 249:1–14
- OHLEMILLER KK, DAHL AR, GAGNON PM (2010a) Divergent aging characteristics in CBA/J and CBA/CaJ mouse cochleae. *J Assoc Res Otolaryngol* doi:10.1007/s10162-010-0228-1
- OHLEMILLER KK, ROSEN AD, GAGNON PM (2010b) A major effect QTL on chromosome 18 for noise injury to the mouse cochlear lateral wall. *Hear Res* 260:47–53
- OKAMOTO Y, HOYA N, KAMIYA K, FUJII M, OGAWA K, MATSUNAGA T (2005) Permanent threshold shifts caused by acute cochlear mitochondrial dysfunction is primarily mediated by degeneration of the lateral wall of the cochlea. *Audiol Neuro-Otol* 10:220–233
- OU HC, HARDING GW, BOHNE BA (2000a) An anatomically based frequency-place map for the mouse cochlea. *Hear Res* 145:123–129
- OU HC, BOHNE BA, HARDING GW (2000b) Noise damage in the C57BL/CBA mouse cochlea. *Hear Res* 145:111–122
- SANTI PA, DUVALL AJ (1978) Stria vascularis pathology and recovery following noise exposure. *Otolaryngology* 86:354–361
- SAUTTER NB, SHICK EH, RANSOHOFF RM, CHARO IF, HIROSE K (2006) CC chemokine receptor 2 is protective against noise-induced hair cell death: studies in CX3CR1^{+/GFP} mice. *J Assoc Res Otolaryngol* 7:361–372
- SCHMIEDT RA, LANG H, OKAMURA H, SCHULTE BA (2002) Effects of furosemide applied chronically to the round window: a model of metabolic presbycusis. *J Neurosci* 22:9643–9650
- SEWELL W (1984) The effects of furosemide on the endocochlear potential and auditory nerve fiber tuning curves in cats. *Hear Res* 14:305–314
- SHI X, NUTTALL AL (2007) Expression of adhesion molecular proteins in the cochlear lateral wall of normal and PARP-1 mutant mice. *Hear Res* 224:1–14
- SPICER SS, SCHULTE BA (2005a) Pathologic changes of presbycusis begin in secondary processes and spread to primary processes of strial marginal cells. *Hear Res* 205:225–240
- SPICER SS, SCHULTE BA (2005b) Novel structures in marginal and intermediate cells presumably relate to functions of basal versus apical strata. *Hear Res* 200:87–101
- SPICER SS, SAMUEL S, SCHULTE BA (1996) The fine structure of spiral ligament cells relates to ion return to the stria and varies with place-frequency. *Hear Res* 100:80–100
- SYKA J, MELICHAR I, ULEHLOVA L (1981) Longitudinal distribution of cochlear potentials and the K⁺ concentration in the endolymph after acoustic trauma. *Hear Res* 4:287–298
- ULEHLOVA L (1983) Stria vascularis in acoustic trauma. *Arch Otorhinolaryngol* 237:133–138
- WANG Y, HIROSE K, LIBERMAN MC (2002) Dynamics of noise-induced cellular injury and repair in the mouse cochlea. *J Assoc Res Otolaryngol* 3:248–268
- WANGEMANN P (2002) K⁺ recycling and the endocochlear potential. *Hear Res* 165:1–9
- WANGEMANN P (2006) Supporting sensory transduction: cochlear fluid homeostasis and the endocochlear potential. *J Physiol* 576(1):11–21
- WARD WD, DUVALL AJ (1971) Behavioral and ultrastructural correlates of acoustic trauma. *Ann Otol* 80:881–896
- YAMASOBA T, KONDO K, MIYAJIMA C, SUZUKI M (2003) Changes in cell proliferation in rat and guinea pig cochlea after aminoglycoside-induced damage. *Neurosci Lett* 347:171–174
- YAMASOBA T, GOTO Y, KOMAKI H, MIMAKI M, SUDO K, SUZUKI M (2006) Cochlear damage due to germanium-induced mitochondrial dysfunction in guinea pigs. *Neurosci Lett* 395:18–22